Josephson tunneling of anisotropic high-T_c *d*-wave junctions with tilted *ab*-plane $YBa_2Cu_3O_{7-y}$ electrodes

H. Arie, K. Yasuda, H. Kobayashi, and I. Iguchi
Department of Applied Physics and CREST, Tokyo Institute of Technology, 2-12-1 Oh-okayama, Meguro-ku, Tokyo 152-8551, Japan

Y. Tanaka
Department of Applied Physics, Nagoya University, Furo-cho, Chikusa-ku, Nagoya 464-8603, Japan

S. Kashiwaya
Electrotechnical Laboratory, 1-1-4 Umezono, Tsukuba 305-0045, Japan
(Received 12 October 1999; revised manuscript received 14 March 2000)

We report measurements on high-T_c $YBa_2Cu_3O_{7-y}$ (YBCO) Josephson ramp-edge junctions with different *ab*-plane orientation electrodes relatively rotated by 45°. The ramp-edge junctions with different crystal angles against the interface boundary are fabricated on an MgO(100) substrate using a CeO_2 seed-layer technique. The Shapiro steps under microwave irradiation of 9 GHz appear qualitatively different for different crystal angles, which supports the *d*-wave nature of a YBCO superconductor. The magnetic-field dependence of the Josephson maximum current shows a Fraunhofer-like pattern, which is consistent with the calculated result for the *d*-wave junctions. The temperature dependencies of the maximum Josephson current for different angle geometry fall off rapidly with increasing temperature and deviate much from the conventional *s*-wave Ambegaokar-Baratoff prediction. The results are in good qualitative agreement with the calculated results based on the *d*-wave pairing symmetry taking the presence of the zero energy state into account. The observed angle dependencies clearly indicate that the angle-dependent Josephson current really exists.

I. INTRODUCTION

The symmetry of the wave function of Cooper pairs for high-T_c oxide superconductors has recently been attracting considerable attention among many researchers. It is very important to clarify the pairing symmetry in order to understand the physical properties of high-T_c oxide superconductors. In a series of experiments conducted in recent years, evidence was gathered suggesting that high-T_c oxide superconductors have an anisotropic $d_{x^2-y^2}$-wave symmetry.[1–5] In one of these experiments, Wollman *et al.* demonstrated the *d*-wave pairing symmetry of a high-T_c $YBa_2Cu_3O_{7-y}$ (YBCO) superconductor by measuring the magnetic-field dependence of the maximum Josephson current for a corner-type junction made of a YBCO single crystal and a Pb film.[1,2] The maximum Josephson current exhibited a diplike structure around the zero magnetic field, in contrast to the conventional *s*-wave magnetic diffraction pattern. Iguchi and Wen also observed a similar behavior for a planar-type YBCO/insulator/Pb Josephson junction.[3] Later, it was pointed out that the pairing symmetry of high-T_c superconductors may not be pure *d* wave, but the mixture of *d*-wave and *s*-wave components.[6,7] Since high-T_c superconductors have an anisotropic structure, it has been argued that the *s*-wave component exists along the *c*-axis direction or the *s*-wave component is induced by orthorhombic structure in the case of YBCO. However, it is now generally accepted that high-T_c superconductors predominantly have a *d*-wave pairing symmetry.

In anisotropic *d*-wave symmetry, the phenomena in the high-T_c Josephson junction become different from those of the conventional *s*-wave superconductor. These phenomena would be strongly dependent on the angle between the crystal orientation of a superconductor and the junction boundary interface. For example, the Josephson current is closely related to the crystal orientation angles α and β as shown in Fig. 1(a), where α and β are the angles between the crystal orientation of two different electrodes and the direction normal to the boundary interface and α_0 is the relative angle between the crystal orientations of two electrodes. According to the theory by Sigrist and Rice,[8] the maximum Josephson current depends on the angles α and β in the following way:

$$I_C = A \cos 2\alpha \cos 2\beta. \tag{1}$$

Equation (1) shows that the maximum value of the Josephson current differs for the different sets of values of α and β.

Later, it was pointed out that a novel interference effect of the quasiparticles appears near the surface and the interface where the pair potential changes sign on the Fermi surface, which leads to the formation of a zero energy state (ZES).[9] The presence of the ZES influences the transport properties of the tunnel junction significantly. This ZES is detectable as the conductance peak in the tunneling characteristics.[10–12] The formation of the ZES has been actually detected in several tunneling spectroscopy experiments.[13–23] The influence of the ZES formation on the dc Josephson current in a singlet unconventional superconductor has been studied theoretically, as shown in the description in the next section,[24–26] in which the temperature dependence of the maximum Josephson current appears to be quite anomalous and strongly depends on the angle between the crystal orientation and the interface boundary. It falls off more rapidly for a

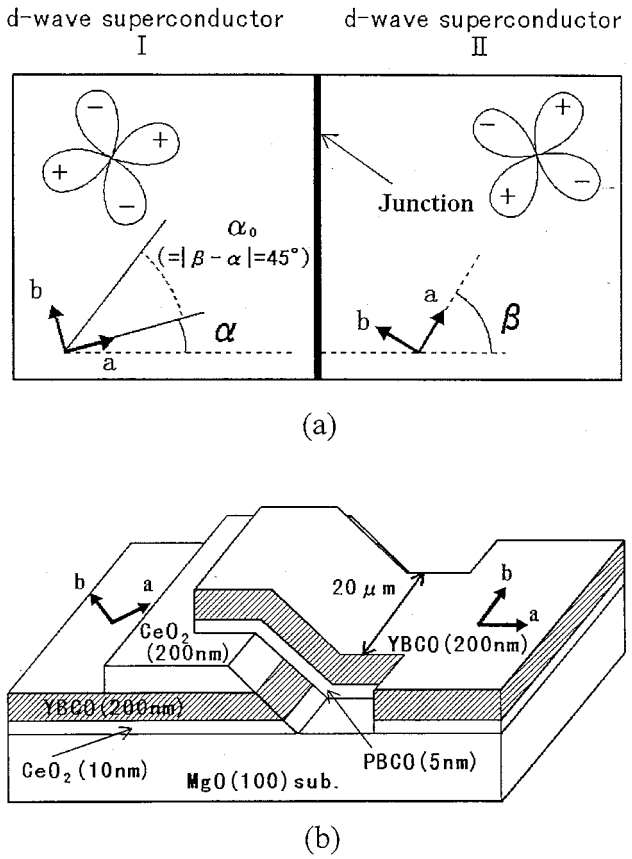

FIG. 1. (a) Schematic geometry of the junction. The clover-shaped *d*-wave order parameters are fixed to the crystal lattices of two electrodes. α and β are the angles between the normal of the interface and the crystal lattice on the left and right sides, respectively. (b) Schematic geometry of the YBCO/PBCO/YBCO ramp-edge junction with tilted *ab*-plane electrodes.

$d_{x^2-y^2}$-wave than for an *s*-wave case for the low impedance junctions with low barrier parameter. For the high impedance junctions, they exhibit more complicated behavior in which the maximum Josephson current once falls off to zero or a minimum point at a certain temperature below T_c, then increases and finally drops to zero again at T_c. Experimentally, however, it is very difficult to fabricate high-T_c Josephson junctions with high impedance. Hence we consider that this anomalous temperature dependence will not be observable. We mention that the properties of *d*-wave Josephson junctions also appear in the microwave and magnetic-field measurements, but they do not appear so much remarkably as compared with the temperature dependence of the maximum Josephson current.

In studies of high-T_c Josephson junctions, there have been many measurements on the properties of the Josephson current using a bicrystal junction,[27,28] a ramp-edge junction,[29,30] or a step-edge junction.[31] There is also an intensive review article on the temperature dependence of the Josephson maximum current for high-T_c SNS junctions.[32] Although there exist several reports on the *d*-wave effect of the Josephson junctions,[33–36] no angle-resolved measurement of the junction properties seems to have been carried out. It has been reported that the bicrystal grain-boundary is naturally rough due to the original crystal defects of the substrate which will remarkably affect the *d*-wave properties of the junction.[37]

According to the ZES theory, as stated above, various interesting properties of the Josephson junction between *d*-wave superconductors are expected when the superconductor electrodes are relatively rotated by 45°, i.e., $\alpha_0 = 45°$. We thus fabricated asymmetric ramp-edge junctions ($\alpha_0 = 45°$ and various β) by rotating the in-plane orientation angle of one superconductor electrode using the seed-layer technique shown in Fig. 1(b). Note that, with our sample geometry, the essential range of β is 0°–22.5° ($=\pi/8$), and $\beta = 30°$ is equivalent to $\beta = 15°$ by considering the geometry taken in Fig. 1(a). It has been recently demonstrated that the ramp-edge junction technique is very powerful for studying the angular dependence of the tunnel current in high-T_c *d*-wave superconductors.[22] The fabricated Josephson junctions used here were quite reproducible. The temperature dependence of the maximum Josephson current and the microwave irradiation properties appeared quite anomalous for these junctions and are in good agreement with the calculated results based on the recent *d*-wave theory.

II. THEORETICAL MODEL

By applying the ZES-based Josephson tunneling theory to the two-dimensional superconductors,[24,25] the Josephson current at a finite temperature T is given by

$$R_N I(\varphi) = \frac{\pi \overline{R}_N k_B T}{e} \left\{ \sum_{\omega_n} \int_{-\pi/2}^{\pi/2} F(\theta, i\omega_n, \varphi) \times \sin\varphi \sigma_N \cos\theta d\theta \right\}, \tag{2}$$

where $\omega_n = 2\pi k_B T(n+\frac{1}{2})$, $\varphi = \varphi_L - \varphi_R$, and θ is the incident angle of the electronlike quasiparticles normal to the interface boundary. The external phase of the two superconductors φ_L and φ_R is measured from their crystal axes as in Refs. 24 and 25. σ_N is the normal conductivity of the junction, R_N denotes the normal resistance of the junction, k_B is the Boltzmann constant, and e is the electronic charge. The detailed form of the function $F(\theta, i\omega_n, \varphi)$ has been given in Ref. 24. We adopt the delta-function model to express the tunnel insulating barrier. Then $\overline{R}_N$ and σ_N are expressed as

$$\overline{R}_N^{-1} = \int_{-\pi/2}^{\pi/2} \sigma_N \cos\theta d\theta, \quad \sigma_N = \frac{1}{1+Z_\theta^2},$$

$$Z_\theta = \frac{Z}{\cos\theta}, \quad Z = \frac{mH}{\hbar^2 k_F}, \tag{3}$$

where Z is the barrier parameter, H denotes the strength of the δ-function barrier, k_F is the wave number at the Fermi surface, m is the electron mass, and h is the Planck's constant divided by 2π. The result is applicable to the case of arbitrary barrier height and for spin singlet superconductors with any symmetry.

In the actual calculations, we can take into account the broadening of the lifetime of quasiparticles by substituting ω_n with $\omega_n + \mathrm{sgn}(\omega_n)\gamma$, where γ is the parameter of lifetime

broadening. Hereafter, we will calculate the Josephson current in the *d*-wave superconductor/insulator/*d*-wave superconductor ($d/I/d$) junction, where the order parameters are described by $\Delta_L(\theta_\pm)=\Delta_d\cos[2(\theta\mp\alpha)]$ and $\Delta_R(\theta_\pm)=\Delta_d\cos[2(\theta\mp\beta)]$. The quantities α and β are the angles between the normal vector of the superconductor to the crystal axes of the left and right superconductors, respectively. For example, for $\alpha=\beta=0$, $R_NI(\varphi)$ can be expressed as

$$R_NI(\varphi)=\frac{\pi\overline{R_N}}{e}\int_{-\pi/2}^{\pi/2}\frac{\Delta_d(T)\cos 2\theta\sigma_N\cos\theta\sin\varphi}{2\sqrt{1-\sigma_N\sin^2(\varphi/2)}}\times\tanh\left[\frac{\Delta_d(T)\cos 2\theta\sqrt{1-\sigma_N\sin^2(\varphi/2)}}{2k_BT}\right]d\theta, \tag{4}$$

where $\Delta_d(T)$ is the gap parameter of the *d*-wave superconductor. The temperature dependence of the maximum Josephson current is similar to that of the ordinary Ambegaokar-Baratoff (AB) theory.[38] On the other hand, for $\alpha=-\beta=\pi/4$, the resulting $R_NI(\varphi)$ becomes

$$R_NI(\varphi)=-\frac{\pi\overline{R_N}}{e}\int_{-\pi/2}^{\pi/2}\frac{f(T,\theta)\sin\varphi}{2\sqrt{\sigma_N}\sin(\varphi/2)}\times\tanh\left[\frac{f(T,\theta)\sin(\varphi/2)\sqrt{\sigma_N}}{2k_BT}\right]\sigma_N\cos\theta d\theta, \tag{5}$$

where $f(T,\theta)=\Delta_d(T)\sin(2\theta)$ and $\sqrt{\sigma_N}|f(T,\theta)|\ll 2k_BT$, $R_NI(\varphi)$ is proportional to the inverse of T.[25,26] In other words, the Josephson current is enhanced as temperature is reduced. This anomalous behavior originates from the existence of ZES at the interfaces of both the left and right superconductors. The ZES appears for any finite value of Z and disappears for $Z=0$. For large Z, it appears as bound states, but with decreasing Z, it changes to a kind of resonant state which finally disappears for $Z=0$. It is necessary to point out that the low-impedance junctions are not directional in transmission, although the magnitude of the Josephson current still depends on the junction orientation.

In the intermediate regime, nonmonotonous temperature dependence of the maximum Josephson current is expected for a small magnitude of σ_N. The Sigrist-Rice result [Eq. (1)] is obtained when only the $\theta=0$ component of $F(\theta,i\omega_n,\varphi)$ in the integral of Eq. (2) is taken into account. The above formula allows us to calculate the temperature dependence and magnetic-field dependence of the maximum Josephson current for our experimental angle geometry ($\alpha_0=45°$ and $\beta=0°-30°$) for the various values of the barrier parameter Z, as shown in the figures later.

III. EXPERIMENTAL

YBCO thin films were grown using a pulsed laser deposition (PLD) method. The detailed fabrication processes of the ramp-edge junctions are described as follows. First, the MgO(100) substrates were annealed in the atmosphere at 1000 °C for 10 h for cleaning the substrate surface. With this process, the step terrace in the (100) plane became observable, and the surface condition was considerably improved.[39,40] Then, a multilayer film of CeO_2(200 nm)/YBCO(200 nm)/CeO_2(10 nm) was grown *in situ* onto the substrate at 790 °C. The bottom CeO_2 layer was the seed layer for rotating the in-plane orientation of the YBCO crystal by 45°. Next, the patterning process was carried out by photolithography and Ar ion milling of 250 eV beam voltage. The ion milling of the films was done by mounting the sample on a water-cooled sample holder. A sequential process of 3 min. milling time and 5 min. interval was taken to avoid possible heating effects. In this process, the ion-gun axis and the substrate were positioned at an angle of 45°, and the ramp-edge structure was thus formed. The junctions of various angles β were fabricated by patterning the ramp-edge line in an arbitrary direction. The edge surface was cleaned by 150 eV ion milling after the photoresist was removed, and then the sample was transferred from the milling chamber to the PLD chamber by a load-lock technique. Subsequently, a bilayer film of YBCO(200 nm)/$PrBa_2Cu_3O_{7-y}$(PBCO)(5 nm) was deposited *in situ* at 750 °C, where PBCO served as a barrier layer. Thereafter, again by photolithography and the Ar ion-milling technique, the counter electrode was patterned. The junction width was 20 μm. Finally, the sample was annealed in order to recover the damage by Ar ion milling. The junctions thus fabricated are shown in Fig. 1(b).

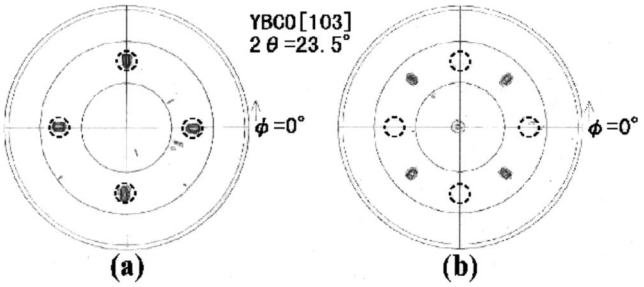

FIG. 2. X-ray diffraction pole figures corresponding to YBCO[103] peak for (a) YBCO/MgO(100) and (b) YBCO/CeO_2/MgO(100) layered structures. The results indicate that YBCO crystal lattice grows on MgO(100) cube on cube, while it grows on CeO_2/MgO(100) with the in-plane orientation rotated by 45°.

In Fig. 2, the results on the x-ray diffraction (XRD) pole figures for YBCO/MgO- and YBCO/CeO_2/MgO-layered structures are shown. In the XRD pole-figure measurement, the peak corresponding to the YBCO[103] direction was used. In the measurements of the usual $\theta/2\theta$ scanning, only [00l] peaks (l: integer) were found. The full width at half maximum of the peak was about 0.4°, indicating a good *c*-axis orientation. The peaks should appear in the dotted-line circles in the figure when MgO and YBCO crystals are grown cube on cube. For the YBCO/MgO structure, the cube-on-cube growth can be observed, while for the YBCO/CeO_2/MgO-layered structure, the peaks appeared at the points rotated 45° from them. The YBCO[103] peaks had four-time symmetry in each pole figure, which indicates that each YBCO thin film is twin-free. We conclude that the in-plane orientation of the two YBCO thin films was relatively rotated by 45°. The ramp-edge surface was investigated using an atomic force microscope (AFM). The mean square roughness (RMS) was about 3 nm. We note, however, that the dominant roughness arose from the local outgrowth

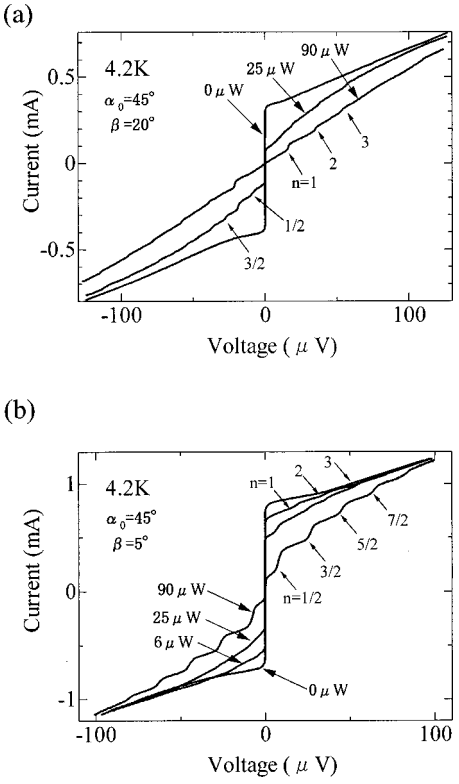

FIG. 3. Current-voltage characteristics with and without microwave irradiation of 9 GHz at 4.2 K for the junctions with (a) $\alpha_0 = 45°$, $\beta = 20°$ and (b) $\alpha_0 = 45°$, $\beta = 5°$.

grains, but the film surface was otherwise quite smooth. The local outgrowth grains produced by Ar ion milling may be considered as the Y-rich/Cu-poor phase according to recent research on the ramp-edge surface.[41–43] The edge angle was 15°–30°. We have prepared many samples with different crystal angles ($\alpha_0 = 45°$; $\beta = 0°$, 5°, 10°, 20°, and 30°) against the interface boundary.

IV. RESULTS AND DISCUSSION

We mainly performed the measurements of the temperature dependence of the maximum Josephson current since the difference between the *d*-wave and the *s*-wave junction properties appear in this characteristic remarkably. Some data on the magnetic-field dependence of the maximum Josephson current and the microwave irradiation properties of the junction characteristics were also recorded. The critical temperatures (T_c) of YBCO thin films grown on an MgO substrate and a CeO_2/MgO bilayer were around 80 K. The junction resistances were low, ranging from 0.2 to 0.8 Ω. The critical current density of YBCO thin films was 1×10^7 Å/cm^2 at 4.2 K, and the Josephson current of junctions vanished at 70–80 K. The current-voltage characteristics exhibited a resistively shunted junction (RSJ-) like behavior. The junction resistance (R_N) was almost independent of the temperature, and the $I_C R_N$ product was 0.3 to 0.8 mV at 4.2 K.

First, we present the measurements on the microwave irradiation properties on the junctions. Figure 3 shows the current-voltage characteristics with and without microwave irradiation of the frequency $f = 9$ GHz for asymmetric ramp-edge junctions with different crystal angles at 4.2 K. Figure 3(a) corresponds to the junction of $\alpha_0 = 45°$, $\beta = 20°$, while Fig. 3(b) corresponds to that of $\alpha_0 = 45°$, $\beta = 5°$. In Fig. 3(a), the microwave steps appeared at integer and half-integer multiples of the voltage (18.6 μV), satisfying the Josephson voltage-frequency relation $f/V = 483$ GHz/mV (f: frequency). On the contrary, in Fig. 3(b), they appeared at integer multiples of the voltage for small microwave power, whereas they appeared only at $n = 0, \pm\frac{1}{2}, \pm\frac{3}{2}, \pm\frac{5}{2}\ldots$, for large power. The remarkable behavior observed is never expected for conventional *s*-wave superconductors and is considered to be a property of the *d*-wave superconductors. According to Tanaka[44] and Yip,[45] it has been shown from the arguments on the pairing symmetry that the $\sin\varphi$ component of the Josephson current completely vanishes for the angle configuration of $\alpha_0 = 45°$, $\beta = 0°$, and only the $\sin 2\varphi$ component survives, yielding half-integer multiple steps. As the angle β becomes larger, the contribution of the $\sin\varphi$ component increases, and the irradiation properties exhibit the mixed behavior of $\sin\varphi$ and $\sin 2\varphi$. The observed behavior is generally consistent with this picture. For $\beta = 20°$, the significant contribution of the $\sin\varphi$ component yielded the appearance of clear-integer multiple steps in addition to half-integer multiple steps. Concerning the case of $\beta = 5°$, which is very close to the case of $\beta = 0°$ and in which the $\sin 2\varphi$ term is considered to be dominant, the half-integer steps and the $n = 0$ step were observable. Unfortunately, we could not analyze the observed characteristics further in the absence of detailed Shapiro-step calculations based on the *d*-wave model.

The maximum Josephson current also responded to an externally applied magnetic field. Figure 4 shows the observed Fraunhofer-like patterns for the magnetic field applied normal (a) and parallel (b) to the substrate surface for different samples [(a): $\alpha_0 = 45°$; $\beta = 30°$ and (b): $\alpha_0 = 45°$; $\beta = 0°$]. In Fig. 4(a), the Fraunhofer pattern appeared in the large junction regime.[44] The result is quite reasonable since the junction width ($w = 20\,\mu$m) is much greater than the estimated Josephson penetration depth λ_J of 2.4 μm obtained by using a Josephson current density of $J_c = 1.5 \times 10^4$ A/cm^2, a barrier thickness t of 5 nm, and a penetration depth λ of 0.14 μm. Theoretically, the scale parameter which characterizes the maximum Josephson current vs. the external magnetic field is the lower critical field which is of the order of a few tens of G for YBCO, consistently with the observed behavior. On the other hand, for Fig. 4(b), a periodic structure is seen, which is again reasonable since the effective junction width ($w \fallingdotseq 0.4\,\mu$m: ramp-edge slope: 30°) is much smaller than the estimated λ_J of 3.4 μm for this junction, suggesting a uniform flow of the Josephson current. The observed period was about 160 G. We have calculated the magnetic-field dependence of the Josephson maximum current for zero barrier *d*-wave junctions, which yielded a qualitatively similar behavior to the conventional *s*-wave Fraunhofer pattern, except that the period Φ_0 was replaced by $\Phi_0/2$. Figure 5 depicts such results of $\alpha_0 = 45°$ and various angles of β. For $\beta = 0°$, the curve shows the standard Fraunhofer pattern with the period $\Phi_0/2$, showing the involvement of the $\sin 2\varphi$ term alone. As β increases, the contribution of the $\sin\varphi$ term increases, and the curve deviates from the standard pattern. The observed period differs from

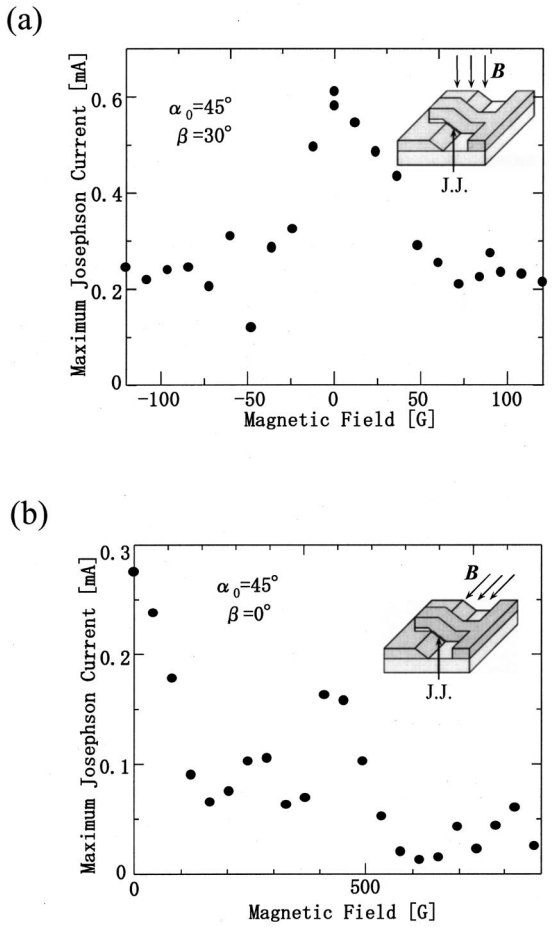

FIG. 4. Dependence of the maximum Josephson current on magnetic field. (a) The case of magnetic field applied normal to the substrate surface. (b) The magnetic field applied parallel to it as shown in the figure. Sample (a) had the angle configuration $\alpha_0 = 45°$, $\beta = 30°$, while sample (b) had the angle configuration of $\alpha_0 = 45°$, $\beta = 0°$.

the calculated value by a factor of about 2, but this factor will be reduced by considering the presence of local outgrowth spots which limit the effective junction area. The result is reasonable in light of the fact that a large discrepancy (of more than one order of magnitude) for the

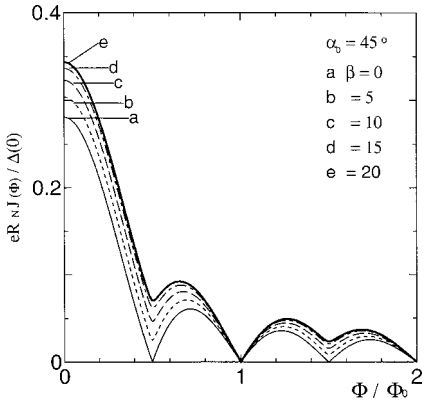

FIG. 5. Calculated magnetic-field dependence of maximum Josephson current for the junctions with $\alpha_0 = 45°$ and various β based on the *d*-wave model. Note that the $\Phi_0/2$ periodic behavior becomes weaker as β increases.

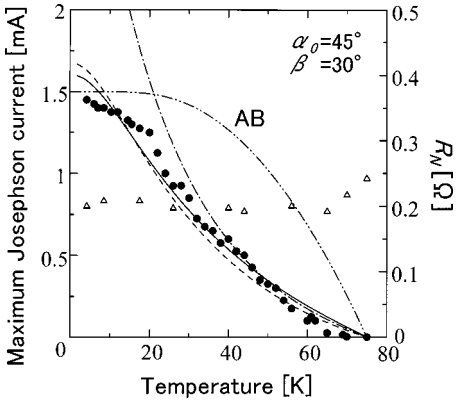

FIG. 6. Maximum Josephson current as a function of temperature for the junction with $\alpha_0 = 45°$ and $\beta = 30°$, together with the temperature dependence of the junction normal resistance R_N. The calculated curves correspond to those based on the *d*-wave theory with [solid line ($Z = 0.5$) and dashed line ($Z = 1$)] and without [dash-dotted line ($Z = 0.5$)] taking the broadening of quasiparticle lifetime into account, respectively. The AB curve corresponds to that of Ambegaokar-Baratoff theory (Ref. 38).

magnetic-field period between the theoretical estimate and the observed data has been generally reported for ramp-edge junctions.[45–49]

The temperature dependences of the maximum Josephson current for the three samples corresponding to the cases $\beta = 10°$, $\beta = 20°$, and $\beta = 30°$ with a fixed angle of $\alpha_0 = 45°$ together with that of the junction normal resistance R_N are shown in Figs. 6–8. Concerning Fig. 6 ($\beta = 30°$), the maximum Josephson current increased monotonically with decreasing temperature and tended to become saturated at low temperatures, while the junction normal resistance was almost constant. In the figure, the results for the *d*-wave theory and the conventional AB theory are also shown.[38] It is clear that the observed result is much deviated from the AB curve. In the calculation based on the theory given in Sec. II, we have fitted the data by the curves with a low barrier height ($Z = 0.5$ and $Z = 1$) since the observed junction resistance was very small. The solid line ($Z = 0.5$) and the dashed line

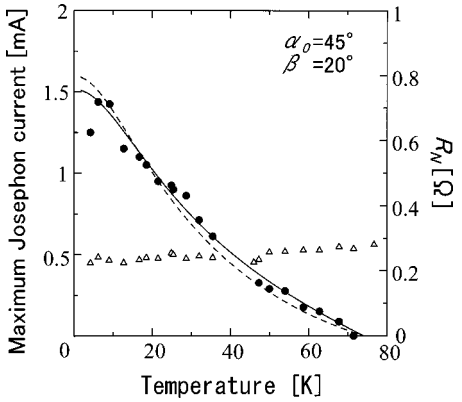

FIG. 7. Maximum Josephson current as a function of temperature for the junction with $\alpha_0 = 45°$ and $\beta = 20°$, together with the temperature dependence of the junction normal resistance R_N. The solid line and the dashed line correspond to the calculated curves for $Z = 0.5$ and $Z = 1.0$ based on the *d*-wave theory with taking the broadening of quasiparticle lifetime into account.

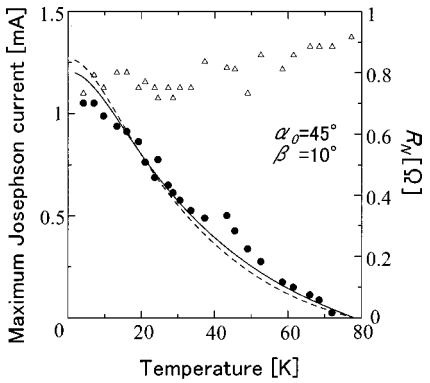

FIG. 8. Maximum Josephson current as a function of temperature for the junction of $\alpha_0=45°$ and $\beta=10°$, together with the temperature dependence of the junction normal resistance R_N. The solid line and the dashed line correspond to the calculated curves for $Z=0.5$ and $Z=1.0$ based on the *d*-wave theory with taking the broadening of quasiparticle lifetime into account, respectively.

($Z=1$) represent the results when taking the broadening of the quasiparticle lifetime ($\gamma=0.2\Delta_d$) into account, while the dash-dotted line ($Z=0.5$) represents that without such effect. It is found that, at low temperatures, the solid line fits the experimental data better than the dash-dotted line, suggesting that the effect of lifetime of quasiparticles is important at low temperatures. Although the data fitting looks a little better for $Z=0.5$ than for $Z=1$, we judge that there is no significant difference between these two curves by considering the scattering of the experimental data points. The strong increase of the maximum Josephson current with decreasing temperature is a manifestation of the existence of ZES's at the interfaces of both the right and left superconductors induced by the *d* wave. In Figs. 7 and 8, the experimental data are also in reasonable agreement with the calculated curves based on the d_{x2-y2}-wave junctions, indicating that the anisotropic Josephson current really exists. It is necessary to point out that the saturating behavior of the maximum Josephson current at low temperatures may not be attributed to the effect of the junction normal resistance since R_N is almost constant in the entire temperature range.

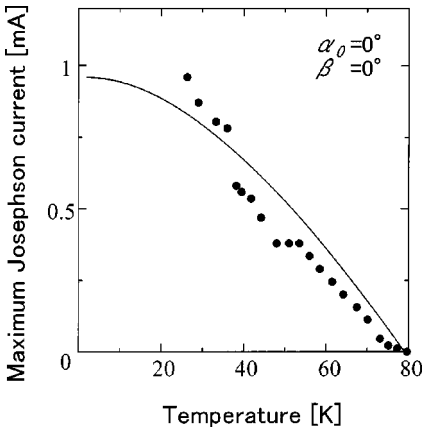

FIG. 9. Temperature dependence of the maximum Josephson current for the ramp-edge junction of $\alpha=\beta=0°$ ($\alpha_0=0°$, $\beta=0°$). The solid line is the calculated curve based on the *d*-wave model for the case of $\alpha=\beta=0°$ with $Z=0.5$ in Ref. 24. Note that, the Ambegaokar-Baratoff behavior is only observable for the junction with large barrier parameter.

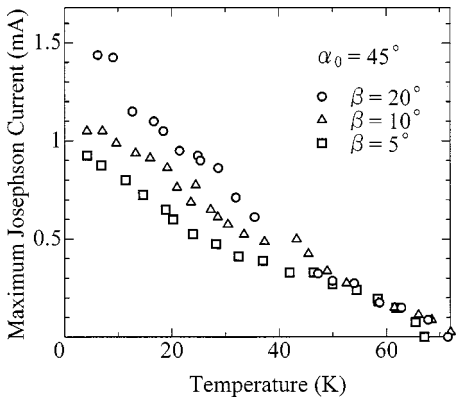

FIG. 10. Temperature dependence of maximum Josephson current for the ramp-edge junctions with $\alpha_0=45°$; $\beta=5°$, 10°, and 20° fabricated simultaneously on the same substrate.

For reference, we have also measured the temperature dependence of the junction of $\alpha=\beta=0$ ($\alpha_0=0°$; $\beta=0°$) whose R_N was about 0.2 Ω. Figure 9 shows the observed result, together with the calculated curve expected from the *d*-wave theory for $Z=0.5$, as shown in Ref. 25. The agreement between the experiment and the theory is reasonably good. Note that, within the framework of the *d*-wave theory, the $\alpha=\beta=0$ case only agrees with the AB result when the barrier parameter Z is large, and the result becomes quite different in the case of zero or low barrier parameter.

Figure 10 shows the temperature dependence of the Josephson maximum current for the ramp-edge junctions of $\alpha_0=45°$; $\beta=5°$, 10°, and 20° simultaneously fabricated by photolithography and the ion-milling technique on the same MgO substrate. The junctions had almost the same quality with resistance ($\fallingdotseq 0.6\Omega$). It was found that the Josephson maximum current was greater for the junction with larger β. Figure 11 shows the calculated temperature dependencies for the junctions of $\alpha_0=45°$; $\beta=0°$, 5°, 10°, 15°, and 20° assuming the barrier parameter $Z=0.5$. The theory also predicts a larger maximum Josephson current for a larger angle β, although the angle dependence is qualitatively similar for low barrier parameter. The observed result was in good qualitative agreement with the theoretical prediction. Inci-

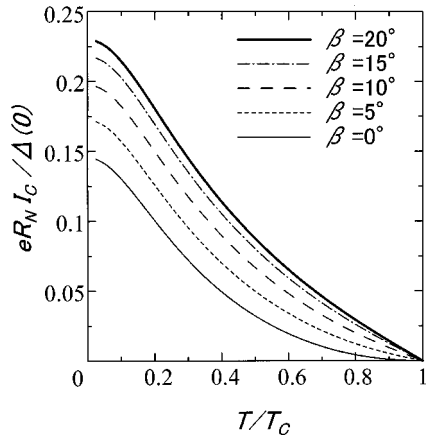

FIG. 11. Calculated curves for the temperature dependence of maximum Josephson current for the *d*-wave junctions with various angle geometry by assuming $Z=0.5$.

dentally, the data demonstrate the existence of the angular dependence in the Josephson current. In the case of $Z=1$, the qualitative features of the curves are almost the same except that the angle-dependence effect becomes slightly stronger. We point out, however, that the observed features rather deviated from the calculated curves in the high-temperature region closer to T_c. They may be attributed to degradation of superconductivity near the junction surface (i.e., order parameter suppression) since the degradation effect becomes remarkable in the high-temperature region.

V. CONCLUSIONS

We have reported the fabrication and transport properties of asymmetric YBCO ramp-edge Josephson junctions in which the in-plane orientation of two YBCO electrode crystals is relatively rotated by 45° using a CeO_2 seed-layer technique. Junctions with different crystal angles against the interface boundary were prepared. The Shapiro steps appeared at integer and/or half-integer multiples of the voltage and satisfied the Josephson voltage-frequency relation, depending on the angle configuration, which was consistent with the *d*-wave picture. The modulation of the Josephson maximum current under a magnetic field normal to the film surface appeared in the large junction regime, while, for a magnetic field parallel to the film surface, it exhibited a normal Fraunhofer pattern, which is consistent with *d*-wave calculations with low barrier parameter. The observed temperature dependencies of the maximum Josephson current were quite different from those expected for the AB theory and are in good qualitative agreement with the calculated results based on the *d*-wave theory taking the zero energy state into account. Although the observed angle dependencies were qualitatively similar for the junctions with low impedance, the results clearly indicate that the angle-dependent Josephson current really exists.

ACKNOWLEDGMENTS

This work has been supported by CREST (Core Research for Evolutional Science and Technology) of Japan Science and Technology Corporation (JST).

[1] D. A. Wollman, D. J. van Harlingen, J. Giapintzakis, and D. M. Ginsberg, Phys. Rev. Lett. **74**, 797 (1995).
[2] D. A. Wollman, D. J. van Harlingen, W. C. Lee, D. M. Ginsberg, and A. J. Leggett, Phys. Rev. Lett. **71**, 2134 (1993).
[3] I. Iguchi and Z. Wen, Phys. Rev. B **49**, 12 388 (1994).
[4] C. C. Tsuei, J. R. Kirtley, C. C. Chi, L. S. Yu-Jahnes, A. Gupta, T. Shaw, J. Z. Sun, and M. B. Ketchen, Phys. Rev. Lett. **73**, 593 (1994).
[5] A. Mathai, Y. Gim, R. C. Black, A. Amar, and F. C. Wellstood, Phys. Rev. Lett. **74**, 4523 (1995).
[6] K. A. Kouznetsov, A. G. Sun, B. Chen, A. S. Katz, S. R. Bahcall, J. Clarke, R. C. Dynes, D. A. Gajewski, S. H. Han, M. B. Maple, J. Giapintzakis, J.-T. Kim, and D. M. Ginsberg, Phys. Rev. Lett. **79**, 3050 (1997).
[7] R. Kleiner *et al.*, Phys. Rev. Lett. **76**, 2161 (1996).
[8] M. Sigrist and T. M. Rice, J. Phys. Soc. Jpn. **61**, 4283 (1992).
[9] C. R. Hu, Phys. Rev. Lett. **72**, 1526 (1994).
[10] S. Kashiwaya, Y. Tanaka, H. Takashima, M. Koyanagi, and K. Kajimura, Phys. Rev. B **51**, 1350 (1995).
[11] S. Kashiwaya, Y. Tanaka, M. Koyanagi, and K. Kajimura, Phys. Rev. B **53**, 2667 (1996).
[12] Y. Tanaka and S. Kashiwaya, Phys. Rev. Lett. **74**, 3451 (1995).
[13] J. Geerk, X. X. Xi, and G. Linker, Z. Phys. B: Condens. Matter **73**, 329 (1988).
[14] M. Furuyama, I. Iguchi, K. Shirai, T. Kusumori, H. Ohtake, S. Tomura, and M. Nasu, Jpn. J. Appl. Phys., Part 2 **29**, L459 (1990).
[15] I. Iguchi and Z. Wen, Physica C **178**, 1 (1991).
[16] J. H. Lesuer, L. H. Green, W. L. Feldman, and A. Inam, Physica C **191**, 325 (1992).
[17] M. Covington, M. Aprili, E. Paraoanu, L. H. Greene, F. Xu, J. Zhu, and C. A. Mirkin, Phys. Rev. Lett. **79**, 277 (1997).
[18] L. Alff, H. Takashima, S. Kashiwaya, N. Terada, Y. Tanaka, M. Koyanagi, and K. Kajimura, Phys. Rev. B **55**, 14 757 (1997).
[19] J. Y. T. Wei, N.-C. Yeh, D. F. Garrigus, and M. Strasik, Phys. Rev. Lett. **81**, 2542 (1998).
[20] S. K. Sinha and K.-W. Ng, Phys. Rev. Lett. **80**, 1296 (1998).
[21] S. Ueno, S. Kashiwaya, N. Terada, M. Koyanagi, Y. Tanaka, and K. Kajimura, J. Phys. Chem. Solids **59**, 2081 (1998).
[22] W. Wang, M. Yamazaki, K. Lee, and I. Iguchi, Phys. Rev. B **68**, 4272 (1999).
[23] O. Nesker and G. Koren, Phys. Rev. B **60**, 14 893 (1999).
[24] Y. Tanaka and S. Kashiwaya, Phys. Rev. B **53**, R11 957 (1996).
[25] Y. Tanaka and S. Kashiwaya, Phys. Rev. B **56**, 892 (1997).
[26] Yu. S. Barash, H. Burkhardt, and D. Rainer, Phys. Rev. Lett. **77**, 4070 (1996).
[27] P. Chaudhari, J. Mannhart, D. Dimos, C. C. Tsuei, C. C. Chi, M. M. Oprysko, and M. Scheuermann, Phys. Rev. Lett. **60**, 1653 (1988).
[28] D. Dimos, P. Chaudhari, and J. Mannhart, Phys. Rev. B **41**, 4038 (1990).
[29] J. Gao, Y. M. Boguslavskij, B. B. G. Klopman, D. Terpstra, R. Wijbrans, G. J. Gerritsma, and H. Rogalla, J. Appl. Phys. **72**, 1 (1992).
[30] C. Horstmann, P. Leinenbach, A. Engelhardt, R. Dittmann, U. Memmert, U. Harttmann, and A. I. Braginski, IEEE Trans. Appl. Supercond. **2**, 2844 (1997).
[31] G. Friedel, B. Roas, M. Romheld, L. Schultz, and W. Jutzi, Appl. Phys. Lett. **59**, 2751 (1991).
[32] K. A. Delin and A. W. Kleinsasser, Supercond. Sci. Technol. **9**, 227 (1996).
[33] J. Mannhart, Hi. Hilgenkamp, B. Meyer, Ch. Gerber, J. R. Kirtley, K. A. Moler, and M. Sigrist, Phys. Rev. Lett. **77**, 2782 (1996).
[34] E. Il'ichev, Z. Zakosarenko, R. P. J. Ijsselsteijn, V. Schultze, H. G. Meyer, H. E. Hoenig, H. Hilgenkamp, and J. Mannhart, Phys. Rev. Lett. **81**, 894 (1998).
[35] Z. G. Ivanov, E. A. Stepantsov, T. Claeson, F. Wenger, S. Y. Lin, N. Khare, and P. Chaudhari, Phys. Rev. B **57**, 602 (1998).
[36] E. Il'ichev, V. Zakosarenko, R. P. J. Ijsselsteijn, H. E. Hoenig, H. G. Meyer, M. V. Fistul, and P. Muller, Phys. Rev. B **59**, 11 502 (1999).

[37] K. Lee and I. Iguchi, Appl. Phys. Lett. **66**, 769 (1995).
[38] V. Ambegaokar and A. Baratoff, Phys. Rev. Lett. **10**, 486 (1963).
[39] M. Naito and H. Sato, Physica C **229**, 1 (1994).
[40] M. Yoshimoto, T. Maeda, K. Shimozono, H. Koinuma, M. Shinohara, O. Ishiyama, and F. Ohtani, Appl. Phys. Lett. **65**, 3197 (1994).
[41] J. G. Wen, N. Koshizuka, S. Tanaka, T. Satoh, M. Hidaka, and S. Tahara, Appl. Phys. Lett. **75**, 2470 (1999).
[42] T. Nagano, S. Inoue, H. Sugiyama, and J. Yoshida (unpublished).
[43] Y. Soutome, T. Fukazawa, A. Tsukamoto, Y. Tarutani, and K. Takagi (unpublished).
[44] Y. Tanaka, Phys. Rev. Lett. **72**, 3871 (1994).
[45] S. Yip, J. Low Temp. Phys. **91**, 203 (1993).
[46] C. S. Owen and D. J. Scalapino, Phys. Rev. **164**, 538 (1967).
[47] L. Antoghazza *et al.*, Phys. Rev. B **52**, 4559 (1995).
[48] B. H. Moeckly and K. Char, Appl. Phys. Lett. **71**, 2526 (1997).
[49] A. Fujimaki *et al.*, IEEE Trans. Appl. Supercond. **9**, 3436 (1999).